PCCP

Accepted Manuscript

ROYAL SOCIETY OF CHEMISTRY

www.rsc.org/pccp

ARTICLE TYPE www. rsc.org/xxxxxx | XXXXXXXX

Lithium Boride Sheet and Nanotubes: Structure and Hydrogen Storage

Hong Zhang,[ab] Jing Wang,[ad] Zhi-Xue Tian,[a] and Ying Liu*[ac]

Received Xth XXXXXXXXXX 20XX, Accepted Xth XXXXXXXXX 20XX
First published on the web Xth XXXXXXXXXX 200X
DOI: 10.1039/b000000x

A new class of Li-B sheets along with the related nanotubes, with Li_2B_5 primitive cell has been designed using first-principles density functional theory. The dynamical stability of the proposed structures was confirmed by calculation of soft phonon modes, and the calculated electronic structures show that all are metallic. The application of both the sheets and nanotubes to hydrogen storage has been investigated and it has been found that both of them can adsorb two H_2 molecules around each Li atom with an average binding energy of 0.152 - 0.194 eV/H_2, leading to a gravimetric density of 10.6 wt%.

1 Introduction

Boron, the fifth element, next to carbon in the periodic table, has numerous and inevitably complicated crystalline phases due to its electron deficiency and thus the tendency to form multicenter bonds. Consequently boron is considered as the second element, along with carbon, that has multiple low-dimensional allotropes. Indeed, as long ago as 1997, I. Boustani[1] suggested that small boron clusters might exhibit quasi-planar structures. These structures were later confirmed experimentally by Wang, Boldyrev and their co-workers[2–4], who also subsequently discovered the structural transition from quasi-planar to double-ring tubular structures for small-sized boron clusters. They were also the first to predict the existence of single-walled boron nanotubes (BNTs).[5,6] In 2004, Ciuparu[7] successfully synthesized pure single-walled boron nanotube structures with diameters on the order of 3 nm and suggested existence of BNTs. Further theoretical studies showed that boron clusters B_n with n$<$ 20, prefer to be planar. For example, B_{12} has the largest gap, 2.0 eV, between the highest occupied and lowest unoccupied molecular orbitals and is therefore predicted to be very stable.[8] When n$>$20, for instance B_{20}, double-ring tubular configurations can form. These configurations can be considered as the embryonic forms of single-walled boron nanotubes.[9] In 2007, on the basis of *ab initio* calculations, a stable hollow cage with the formula B_{80} similar to the well-known carbon based C_{60} was predicted.[10] This prediction has motivated growing interest in seeking new nanostructures of boron such as boron cage molecules,[11–13] boron sheets (BSs)[14–16] and BNTs[17,18]. To date, the exact atomic structure of BSs has not been determined from experiment, except in the form of indirect evidence that the interlayer separation of multi-walled boron nanotubes is 32 nm,[19] which suggests that the interlayer interaction is likely of the van der Waals type rather than one involving covalent bonds. Nevertheless various crystalline structures of buckled and unbuckled monolayer structures of boron including the α-sheet[14,20,21], β-sheet,[14,20] γ-sheet,[15] triangular sheet and grapheme-like hexagonal sheets, have been predicted from previous *ab initio* computations. Much of this work has been motivated by expectations that these structures may have versatile applications in different fields of science and technology, such as electronics, catalysis and energy storage.

Boron nanomaterials, due to their high surface area and light weight, which is even lighter than carbon, have been extensively investigated as potential hydrogen storage media.[22–28] Using density functional calculations, I. Cabria *et al*.[22] found that pure boron nanotubes and sheets cannot adsorb molecular hydrogen as well as pure carbon nanomaterials. Although studies of alkali-metal(AM)-coated boron fullerenes showed that $B_{80}Na_{12}$ and $B_{80}K_{12}$ can store up most to 72 H_2, while the binding energies are only 0.09 eV/H_2.[23] The best theoretical results, obtained for Mg coated B_{80}, yielded a hydrogen capacity of up to 14.2 wt% with an average binding energy of 0.2 eV/H_2 when the GGA approximation was used, and 0.5 eV/H_2 with the LDA.[25] Suleyman Er found that a planar boron sheet can bind AM more strongly than can graphene,[26] leading to markedly increased hydrogen binding energies and storage capacities. In particular, the Li-decorated sheet can contain up to 10.7 wt% of molecular hydrogen with

[a] *Department of Physics, Hebei Normal University, and Hebei Advanced Thin Film Laboratory, Shijiazhuang 050016, Hebei, China. Fax: 86-311-80787338; Tel: 86-311-80787338; E-mail: yliu@hebtu.edu.cn*
[b] *Department of Science, Hebei University of Energeering, Handan 056038, Hebei, China*
[c] *National Key Laboratory for Materials Simulation and Design, Beijing 100083, China*
[d] *State Key Laboratory for Superlattices and Microstructures, Institute of Semiconductors, Chinese Academy of Sciences, Beijing 100083, China*

an average binding energy of 0.15 eV/H_2.[27] Subsequently, Hui An explored the hydrogen storage capacity of the Li-coated zigzag boron nanotubes, which can absorb up to 7.94 wt% hydrogen with an absorption binding energy of 0.12-0.2 eV/H_2.[28] A previous work of our group investigated a series of Li-decorated several novel boron sheets and nanotubes, showed that for Li-decorated boron sheets, each Li atom can adsorb a maximum of $4H_2$ molecules with 7.89 wt% and the hydrogen gravimetric density increases to 12.31 wt% for Li-decorated boron nanotubes.[29] All these results indicate that B-based materials can be considered as promising reversible host materials for hydrogen storage.

In the present paper, two new quasi two dimensional structures composed of Li and B, as well as their corresponding nanotubes have been studied using first-principles density-functional theory. The structural and electronic properties of these structures are first investigated, and their hydrogen storage characteristics are subsequently explored.

2 Computation method

All geometries were assumed to be periodic, and geometry optimizations and electronic structure calculations were based on first principles calculations performed using the Vienna *ab initio* Simulation Package (VASP).[30] The generalized gradient approximation (GGA) in the form of the PW91[31] functional was used for the exchange and correlation interactions. Binding energies of H_2 molecules in similar systems obtained with the PW91 functional are within $\sim$ 20 meV/H_2 of those obtained with the PBE functional.[32] Therefore, we give only the PW91 results in the following. For all elements involved, the basis set was constructed according to projector augmented wave (PAW)[32] methods with a kinetic energy cutoff of 500 eV. In all these calculations, the Hellmann-Feynman force component on each atom was less than 0.01 eV·Å^{-1} and the convergence criteria for the total energy in the self-consistent field interaction was set to 10^{-4} eV. The first Brillouin zone was sampled on the basis of the Monkhorst-Pack special k-point scheme with a grid spacing of 0.04 Å^{-1} for the wave functions and 0.02 Å^{-1} for the density of states (DOS). Since the bonding is based on weak van der Waals (vdW) interactions, for calculating the hydrogen adsorption in the systems considered here, we included the dispersion correction by using the empirical correction scheme of Grimme (DFT + D2),[34] as implemented by Bucko *et al*. for periodic systems.[35] The phonon dispersion along the high symmetry k-point was obtained using the open source package Phonopy.[36]

3 Results and discussion

3.1 Structure of Li_2B_5 sheets and nanotubes

The first new structure, shown in Fig. 1(*a*), is composed of a ten-atom B planar ring decorated with one Li atom on each side of the ring plane, which reduces to the chemical formula Li_2B_5. We refer to it as the Li_2B_5-I sheet. There are four different B-B bond lengths (1.555Å, 1.665Å, 1.768 Å and 1.877 Å) and three different B-Li bond lengths (2.184 Å, 2.394 Å, 3.305 Å) in the structure. According to a previous report on B_3H_3 (D_{3h} symmetry group) which gave the result that the B-B bond distance was always 1.73 Å and the experimental characterization of B=B double bond lengths that vary between 1.57 Å and 1.59 Å, we can conclude that the sheet has both double bonds and single bonds.[37] In addition, the nearest Li-Li distance is 2.824 Å.

In order to understand the stability of the Li_2B_5-I sheet, we calculated the phonon spectra and performed dynamic stability simulations. The phonon spectra in Fig. 1(*b*) show that all their branches have positive frequencies and that no imaginary phonon modes are to be found in the sheet. To further confirm the dynamic stability, we carried out first-principles molecular dynamics simulations with the NVT ensemble at 600 K using time steps of 2 femtoseconds in 3×3 supercells. After 1 picosecond of simulation, we found that the buckled Li_2B_5 sheet had not been disrupted which means that the structure can remain stable at 600 K for at least 1 picosecond.

The band structure of the Li_2B_5-I sheet shown in Fig. 1(*c*) indicates that the curves for the spin-up bands are almost identical to those for spin-down, which indicates that this structure has little magnetic response. Both the band structure and the total DOS show that the sheet is metallic. To understand the interaction between the Li and B atoms, we carried out bader charge analyses which showed that 0.849 electrons transfer from every Li atom to the B atoms, indicating that the Li atoms are ionized and positively charged. This suggests the possibility of molecular hydrogen adsorption via a polarization mechanism. We also calculated the partial density of states (PDOS) shown in Fig. 1(*d*), from which we can see that there is obvious hybridization between the Li and B atoms. The Li atom donates *s* electrons to B, leading to partially filled B *p* orbitals. At the same time, the Li *p* orbitals split under the strong ligand field generated by the B atoms, thus making the B atoms back-donate some electrons to the Li *p* orbitals, resulting in *p*-*p* and *s*-*p* hybridization between Li and B.

If we pull all the Li atoms in the Li_2B_5-I sheet to one side of the boron sheet and then optimize the geometry, a new sheet which we designate Li_2B_5-II is formed. The energy of this structure is 0.03 eV/atom higher than that of the Li_2B_5-I sheet, but the calculated phonon dispersion plots shown in Fig. 2(*b*) suggest that this sheet is stable. In addition, molecular dy-

namics simulations show that at a temperature of 600 K the structure still retains its original form after a 1 picosecond simulation. The band structure and DOS picture in Fig.2(*c*) show that this structure is metallic as was the Li_2B_5-I sheet.

By rolling up the Li_2B_5-II sheet along different axes, we can obtain a series of nanotubes, varying in diameter in the range 4.48-19.59 Å. In what follows, the nanotubes are labeled as (n,0) (n=5,⋯,10) along the $\mathbf{b}_1$ vector and (0,m) (m=5,⋯,10) along the $\mathbf{b}_2$ vector (n, m are the numbers of unit cells along the $\mathbf{b}_1$ or $\mathbf{b}_2$ vectors respectively as shown in Fig.2*a*). After optimizing the geometries of these tubes by minimization of the total energy, we calculated the energies per atom and compared these values to the corresponding values for the original sheet in order to explore the stability of the nanotubes. See Fig. 3. Here, $\Delta E=E_{atom}$(sheet)-E_{atom}(nanotube). The results show that all these nanotubes are more stable than the sheet and that the cohesive energies per atom for the two nanotube types first decrease with the diameter, and then as the diameter further increases, begin to drop and approach that of the sheet. The calculated electronic properties indicate that all the nanotubes are metallic. Several selected typical structures and their corresponding band structures and DOSs are shown in Fig. 4 and Fig. 5, from which, we can see that all the Li atoms in the cross section form regular polygons and that the B atoms form nanotubes approximating circular cylinders.

3.2 Hydrogen molecule adsorption

We choose a unit cell from the Li_2B_5-I sheet to study the interaction of H_2 molecules with our model and set the interlayer distance to be 20 Å which is sufficient to minimize any artificial interlayer interactions. Here, we define the hydrogen adsorption energy (E_{ad}) as $E_{ad}=\{E[(H_2)_{m-n}@Li_2B_5]+nE[(H_2)]-E[(H_2)_m@Li_2B_5]\}/n$, where $E[(H_2)_m@Li_2B_5]$ is the total energy of Li_2B_5-I sheet complex with m hydrogen molecules, and $E[H_2]$ is the energy of an isolated hydrogen molecule.

First of all, we placed the H_2 molecule at several different locations. After relaxing these structures to minimize the energy, it was found that the first H_2 molecule on each Li atom preferred to tilt towards the Li atom and occupied the side right above the Li atom, with a binding energy of 0.221 eV/H_2 (seen in Fig. 6*a*). The H-H distance in the adsorbed H_2 molecule was found to be 0.757 Å, which is larger than that observed in a free H_2 molecule optimized at the same level (0.749 Å). In the case of $(H_2)_4@Li_2B_5$ (in Fig. 6*b*), the second hydrogen was almost on top of the other Li atom, with a interaction energy per hydrogen molecule of 0.165 eV. The H-H bond distances in this case were found to be 0.755 Å and 0.759 Å. When we added a third hydrogen near each Li atom, after relaxing, the hydrogen was found to lie farther away than the second, with a binding energy of only 0.064 eV. This binding energy is out of the ideal hydrogen storage binding range (0.10 - 0.2 eV), so the sheet can only adsorb two hydrogen molecules around each Li atom, resulting in a maximum hydrogen capacity of up to 10.6 wt%. It is larger than 9.22 wt% obtained by Qiang Sun *et. al.*[38] recently, and almost the same as the best result of those previous studies obtained by coating Li atom on boron sheet (10.7 wt %) as we known.[27]

The adsorption energies and some other corresponding parameters are summarized in Table 1. To elucidate the numerical results presented above, we now turn to electronic structure analyses. It is interesting to note that the amount of charge on the Li atoms remains almost constant during the addition of the first H_2 molecules, but there are 0.03 negative electrons on each H_2 molecule. In order to balance the total number of electrons, the electrons on the B atoms must redistribute slightly. However the configuration of the sheet is not changed much, except that the Li-Li distance is stretched from 2.824 Å to 2.856 Å, and the two B-B bonds change from 1.768 Å and 1.877 Å to 1.764 Å and 1.881 Å. Fig. 7 gives the PDOS of all H, Li and B atoms in the sheet after adsorbing one H_2 molecule on each Li. The PDOS in Fig. 7(*a*) indicates that H 2*p* orbitals take part in the hybridization. There is a sharp peak in the H 2*p* orbital at -7.79 eV overlapping with Li 2*p* (2*s*) orbitals for the case of one H_2 molecule adsorbed on each Li, and a small peak of the H 2*s* orbital around -6.8 eV overlapping with Li and B 2*p* (2*s*) orbitals. At the same time, the sharp peak of the Li 2*p*(2*s*) orbitals have moved from -7.38 eV to -7.79 eV compared with that in the pure sheet as shown in Fig. 1(*d*) and the peak around -1.48 eV has been broadened as well as those of the B orbitals. Fig. 7(*b*) shows that as one more hydrogen molecule is adsorbed around each Li atom, the sharp peak of the H *s* orbitals splits as well as the 2*p* orbitals which broadens the hybridized part, so that not only the peaks located at -7.78 eV and -6.69 eV overlap with the Li 2*p*/2*s* orbitals. Some small peaks around -3.18 eV and the Fermi surface also hybridize with the Li 2*s*(2*p*) orbitals, indicating that hybridization is strengthened, consistent with the bader analysis that an additional 0.06 electrons are transferred to the hydrogen molecules. These results show that the binding of the attached H_2 molecules comes from not only the polarization mechanism but also from orbital hybridization, implying that all the substrate material including the B atoms takes part in the hydrogen adsorption.

To explore the hydrogen storage properties of these nanotubes, we choose (0,5), (0,6), and (0,7) nanotubes as samples to study. With the (0,5) nanotube for example, we added additional H_2 molecules close to the Li atoms one by one, and found that H_2 molecules adsorbed nearby Li atoms in one unit cell are likely to reside in different places outside the space between the Li atoms as can be seen in Fig. 8. The calculated results show that the maximum number of H_2 molecules can be adsorbed per Li atom is two, as same as that for the

sheet. In the case of adsorption of one hydrogen molecule on each Li atom, the average distance between H_2 molecules and Li atoms is 1.947 Å with the adsorption energy of 0.222 eV. When there are two hydrogen molecules being adsorbed by each Li atom, the distance between H_2 and Li atom changes from 2.020 Å to 2.327 Å. The binding energy of the second hydrogen reduced to 0.165 eV. In summary, all these three nanotubes can capture two H_2 molecules around each Li atom with binding energies in the range 0.152-0.194 eV/H_2, and the hydrogen capacity is 10.6 wt% , which achieved the U. S. Department of Energy target for the ideal hydrogen storage material; namely, that the gravimetric density of hydrogen should reach 9 wt% by the year 2015.

4 Conclusions

In summary, we have studied a quasi two dimensional planar sheet with the formula Li_2B_5, and have verified its structural stability through both calculation of the phonon frequencies and simulation of the molecular dynamics. The band structure calculation shows that this structure is metallic. From this sheet we obtained another sheet Li_2B_5-II which can be rolled up to give a series of nanotubes, all of which are metallic. The hydrogen adsorption capacity of the sheet and these nanotubes has been explored. The results show that the sheet as well as the nanotubes can adsorb two H_2 molecules on each Li atom, leading to a gravimetric density of 10.6 wt%. Both the polarization mechanism and orbital hybridization contribute to the adsorption of H_2 molecules. The adsorption energy is suitable for hydrogen storage applications at room temperature.

Acknowledgements

We would like to thank Dr. N. E. Davison for his help with the language. This work is supported by the National Natural Science Foundation of China (Grant Nos. 11274089 and 11304076), the Natural Science Foundation of Hebei Province (Grant Nos. A2012205066 and A2012205069), and the Science Foundation of Hebei Education Award for Distinguished Young Scholars (Grant No. YQ2013008). We also acknowledge partially financial support from the 973 Project in China under Grant No. 2011CB606401.

References

1 Boustani I., *Surf. Sci.* **1997**, *370*, 355.
2 Zhai H. J.; Kiran B.; Wang L. S., *Nat. Mater.* **2003**, *2*, 827.
3 Alexandrova A. N.; Boldyrev A. I.; Zhai H. J.; Wang L. S., *Coord. Chem. Rev.* **2006** , *250*, 2811.
4 Galeev T. R.; Chen Q.; Guo J. G.; Bai H.; Miao C. Q.; Lu H. G.; Sergeeva A. P.; Li S. D.; Boldyrev A. I., *Phys. Chem. Chem. Phys.* **2011**, *13*, 11575.
5 Boustani I.; Quandt A., *Europhys. Lett.* **1997**, *39*, 527.
6 Boustani I.; Rubio A.; Alonso J. A., *Phil. Chem. Phys. Lett.* **1999**, *311*, 21.
7 Ciuparu D.; Klie R. F.; Zhu Y.; Pfefferle L., *J. Phys. Chem. B* **2004**, *108*, 3967.
8 Alexandrova A. N.; Boldyrev A. I.; Zhai H. J.; Wang L. S., *Coord. Chem. Rev.* **2006**, *250*, 2811; Zubarev D. Y.; Boldyrev A. I., *J. Comput.Chem.* **2007**, *28*, 251; Huang W.; Sergeeva A. P.; Zhai H. J.; Averkiev B. B.; Wang L. S.; Boldyrev A. I., *Nat. Chem.* **2010**, *2*, 202.
9 Kiran B.; Bulusu S.; Zhai H. J.; Yoo S.; Zeng X. C; Wang L. S., *Proc. Natl. Acad. Sci. USA* **2005**, *102*, 961.
10 Szwacki N. G.; Sadrzadeh A.; Yakobson B. I., *Phys. Rev. Lett. 2007*, *98*, 166804.
11 Wang X., *Phys. Rev. B* **2010**, *82*, 153409.
12 Zhao J.; Wang L.; Li F.; Chen Z., *J. Phys. Chem. A* **2010**, *114*, 9969.
13 De S.; Willand A.; Amsler M.; Pochet P.; Genovese L.; Goedecher S., *Phys. Rev. Lett.* **2011**, *106*, 225502.
14 Tang H.; Ismail-Beigi S., *Phys. Rev. Lett.* **2007**, *99*, 115501.
15 Özdoğan C.; Mukhopadhyay S.; Hayami W.; GüvençZ. B.; Pandey R.; Boustani I., *J. Phys. Chem. C* **2010**, *114*, 4362.
16 Wu X.-J.; Dai J. ; Zhao Y.; Zhuo Z.-W.; Yang J.-L.; Zeng X.-C., *ACS Nano* **2012**, *6*, 7443.
17 Wang J.; Liu Y.; Li Y.-C., *Chem. Phys. Chem.* **2009**, *10*, 3119.
18 Zope R. R.; Baruah T., *Chem. Phys. Lett.* **2011**, *501*, 193.
19 Bezugly V.; Kunstmann J.; Grundkötter-Tock B.; Frauenheim T.; Niehaus T.; Cuniberti G., *ACS Nano* **2011**, *5*, 4997.
20 Tang H.; Ismail-Beigi S., *Phys. Rev. B* **2010**, *82*, 115412.
21 Miller J., *Phys. Today* **2007**, *60*, 20.
22 Cabria I.; López M. J.; Alonso J. A., *Nanotechnology* **2006**, *17*, 778.
23 Li Y.-C.; Zhou G.; Li J.; Gu B.-L.; Duan W.-H., *J. Phys. Chem. C* **2008**, *112*, 19268.
24 Wu G.-F.; Wang J.-L.; Zhang X.-Y.; Zhu L.-Y., *J. Phys. Chem. C* **2009**, *113*, 7052.
25 Li M.; Li Y.-F.; Zhou Z. ; Shen P.-W.; Chen Z.-F., *Nano Lett.* **2009**, *9*, 1944.
26 Süleyman E.; Gilles A. W.; Geert B., *J. Phys. Chem. C* **2009**, *113*, 18962.
27 Li J. L.; Hu Z. S.; Yang G. W., *Chem. Phys.* **2012**, *392*, 16.
28 An H.; Liu C.-S.; Zeng Z., *J. Chem. Phys.* **2011**, *83*, 115456.

29 Wang J.; Zhao H.-Y.; Liu Y., *ChemPhysChem* **2014**, *10*, 3453.
30 Kresse G.; Hafner J., *Phys. Rev. B* **1993**, *47*, 558; Kresse G.; Hafner J., *Phys. Rev. B* **1994**, *49*, 14251; Kresse G.; Furthmüller J., *Phys. Rev. B* **1996**, *54*, 11169.
31 Perdew J. P.; Chevary J. A.; Vosko S. H.; Jackson K. A.; Pederson M. R.; Singh D. J.; Fiolhais C., *Phys. Rev. B* **1992**, *46*, 6671.
32 Süleyman E.; Gilles A. W.; Geert B., *J. Phys. Chem. C* **2009**, *113*, 8997.
33 Blochl P. E., *Phys. Rev. B* **1994**, *50*, 17953; Joubert D., *Phys. Rev. B* **1999**, *59*, 1758.
34 Grimme S., *J Comput. Chem.* **2006**,*27*, 1787.
35 Bučko T.; Hafner J.; Lebègue S.; Ángyán J. G., *J Phys. Chem. A* **2010**, *114*, 11814.
36 Togo A.; Oba F.; Tanaka I., *Phys. Rev. B* **2008**, *78*, 134106. Code available from http://phonopy.sourceforge.net/
37 Kiran B.; Kumar G.; Nguyen M. T.; Kandalam A. K.; Jena P., *Inorg. Chem.* **2009**, *48*, 9965.
38 Wang Y.-S.; Wang F.; Li M.; Xu B.; Sun Q.; Jia Y., *Appli. Surf. Sci.* **2012**, *258*, 8879.

Table 1 The distance between Li and H atom (d_{Li-H_2} in Å), the bond length of H_2 molecules(d_{H-H} in Å), the distance between the nearest Li atoms (d_{Li-Li} in Å) in the sheet and the hydrogen adsorption energy (E_{ad} in eV/H_2) for the $(H_2)_2$@Li_2B_5-I, $(H_2)_4$@Li_2B_5-I configurations depicted in Fig. 6.

system	d_{Li-H_2}	d_{H-H}	d_{Li-Li}	E_{ad}
Li_2B_5-I		0.749	2.824	
$(H_2)_2$@Li_2B_5-I	1.973	0.757	2.856	0.221
$(H_2)_4$@Li_2B_5-I	2.018-2.085	0.755-0.759	2.926	0.165
$(H_2)_6$@Li_2B_5-I	1.968-3.233	0.750-0.756	2.925	0.064

Table 2 The hydrogen adsorption energies (E_{ad} in eV/H_2) and average hydrogen adsorption energies (E_{aad} in eV/H_2) of nanotubes with different numbers of adsorbed H_2 molecules around each Li atom.

	E_{ad}		E_{aad}
	n=1	n=2	
(0,5)	0.222	0.165	0.194
(0,6)	0.204	0.133	0.168
(0,7)	0.193	0.111	0.152

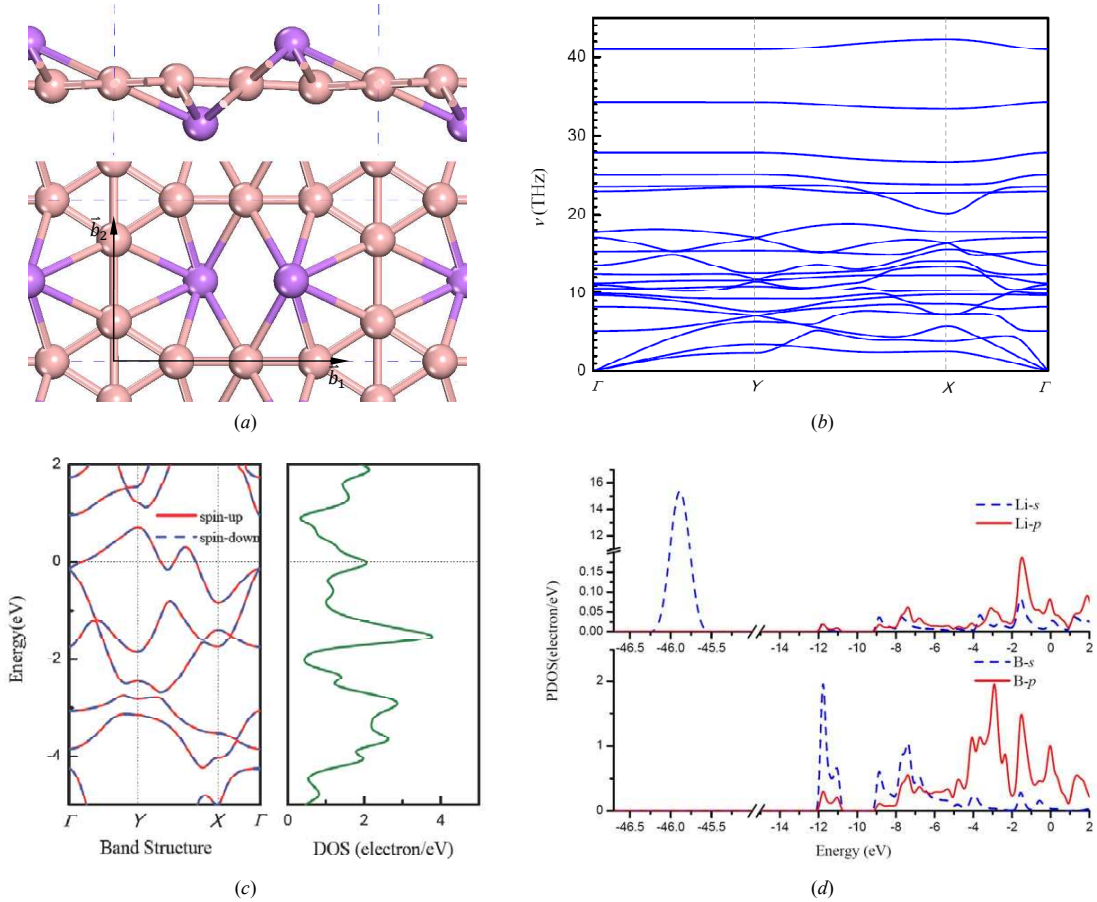

Fig. 1 (*a*) Top and side views of the optimized geometries of Li_2B_5-I 3×3 supercells. (*b*) The phonon spectra of the Li_2B_5-I sheet. (*c*) Calculated band structure along with the density of states (DOS). The Fermi energy is set as zero. , Y and X correspond to the (0, 0, 0), (0, 0.5, 0) and (0.5, 0, 0) k-points, respectively, in the first Brillouin zone. (*d*) The partial density of states (PDOS) of all the Li and B atoms in Li_2B_5-I sheet.

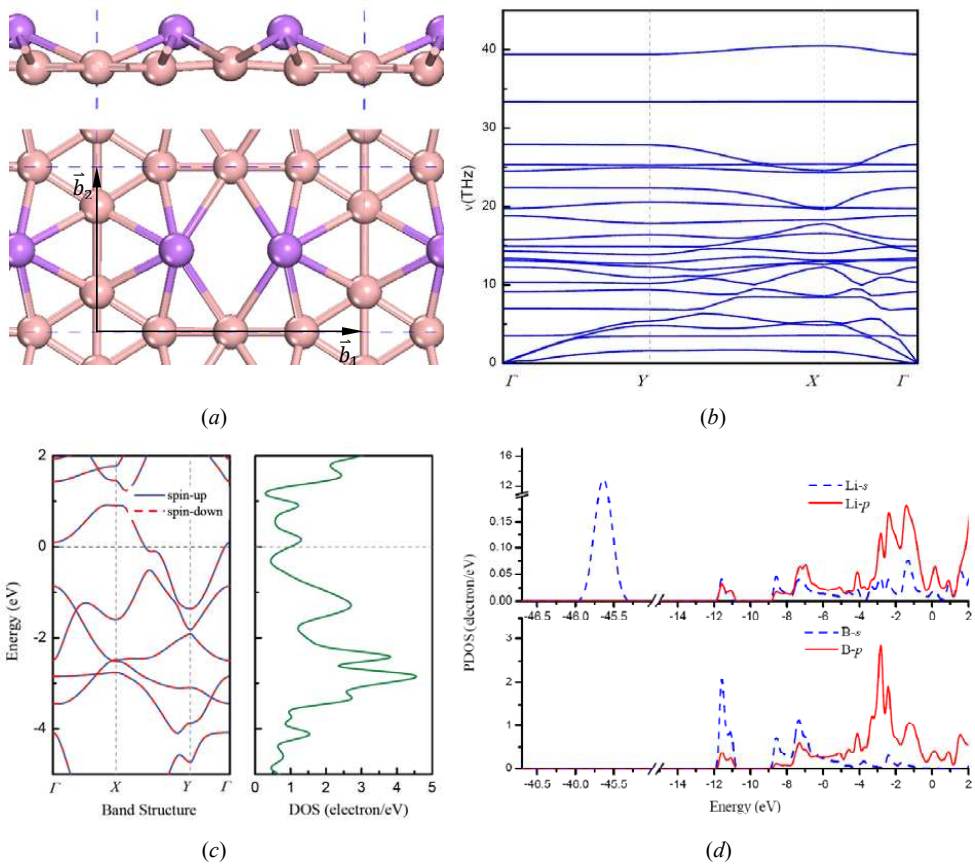

Fig. 2 (*a*) Top and side views of the optimized geometries of Li_2B_5-II 3×3 supercells. (*b*) The phonon spectra of the Li_2B_5-II sheet. (*c*) Calculated band structure along with the density of states (DOS). The k-point lines are the same as those in Figure 1.

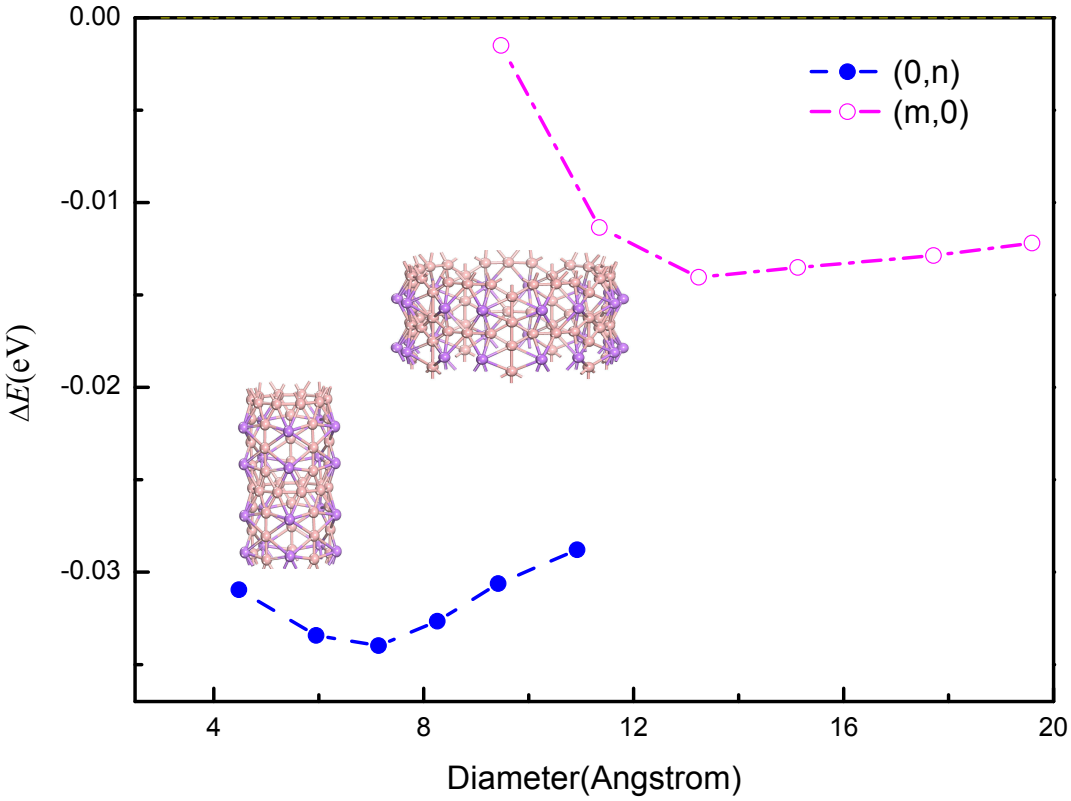

Fig. 3 The total energies per atom of the tubes as a function of the nanotube diameter relative to the Li_2B_5-II sheet.

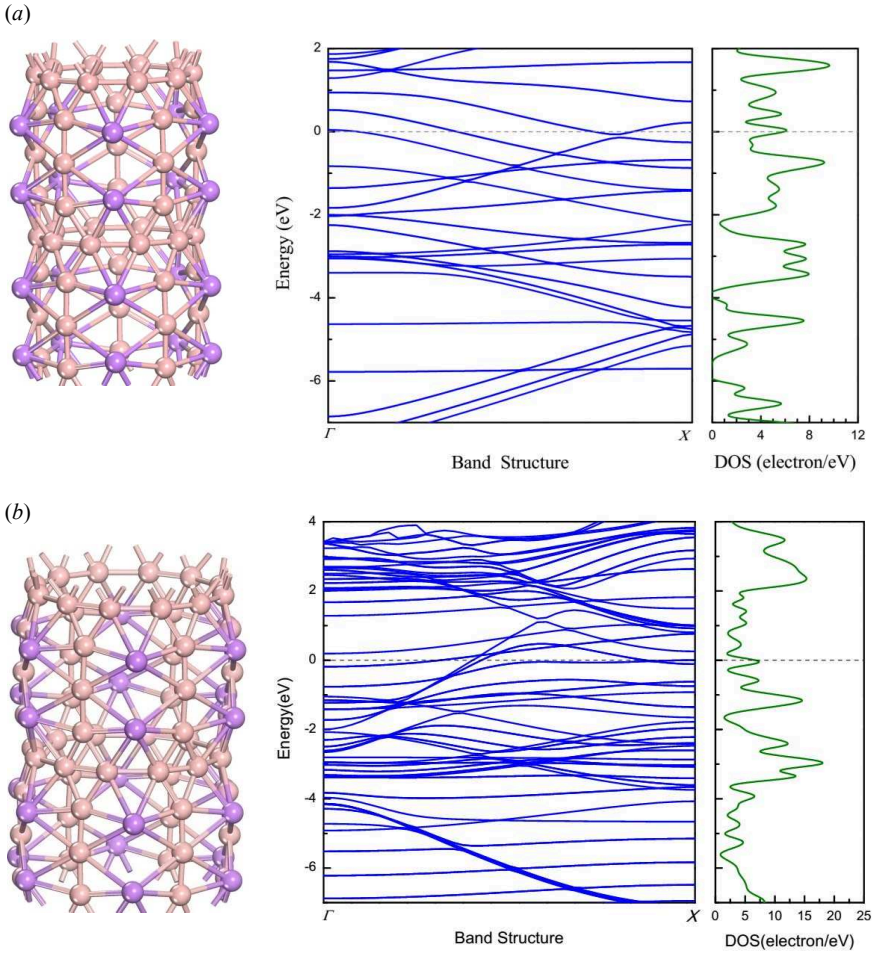

Fig. 4 Side views of the geometric structures, as well as the computed band structures and DOS of nanotubes (*a*) (0,5) and (*b*) (0,8) respectively.

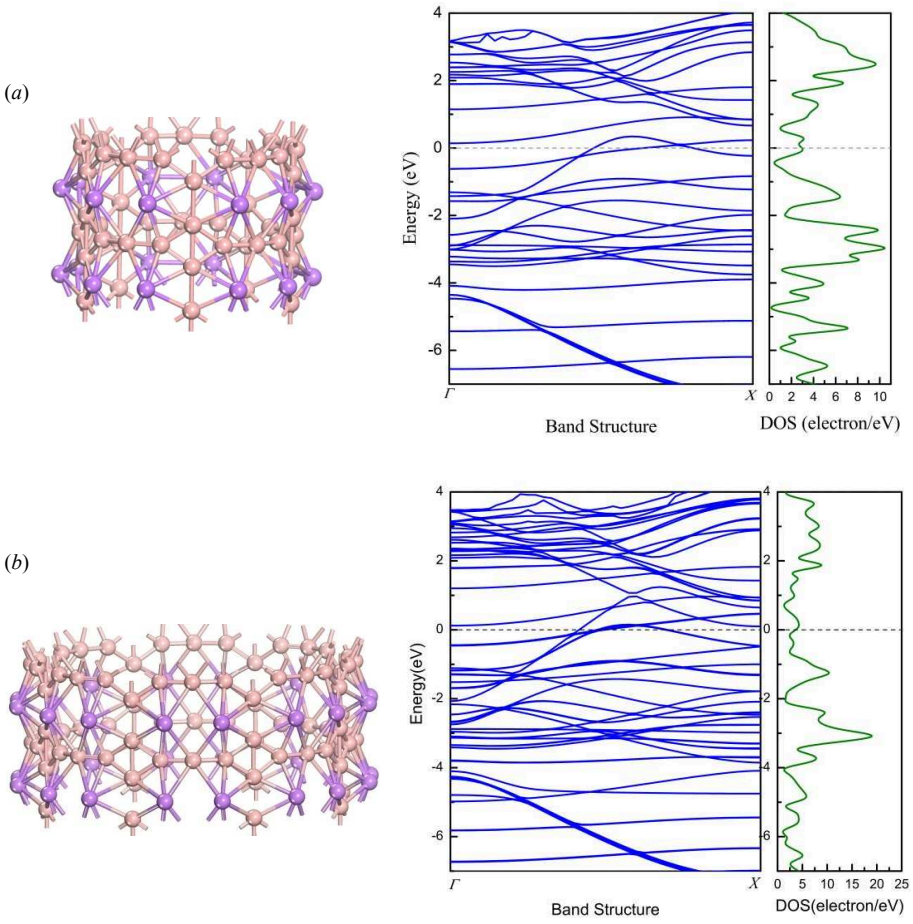

Fig. 5 Side view of the geometric structures, as well as computed band structures and DOS of nanotubes (*a*) (5,0) and (*b*) (6,0) respectively.

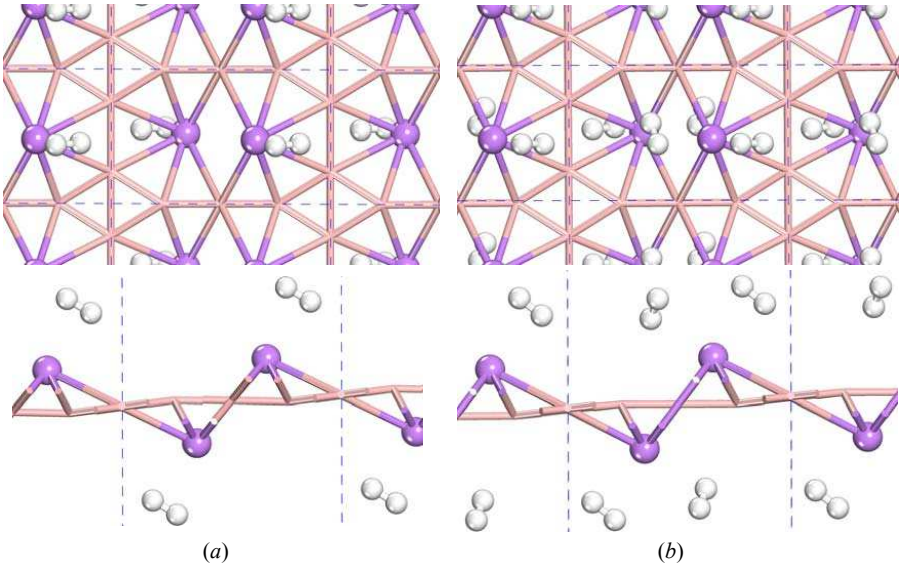

Fig. 6 Top and side views of (*a*) $2H_2$ and (*b*) $4H_2$ molecules bound to a Li_2B_5-I cell. The H atoms bound as hydrogen molecules are shown in white.

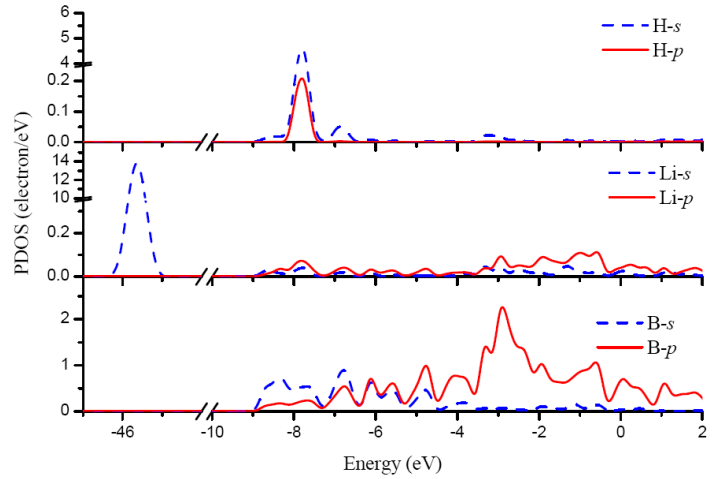

(*a*)

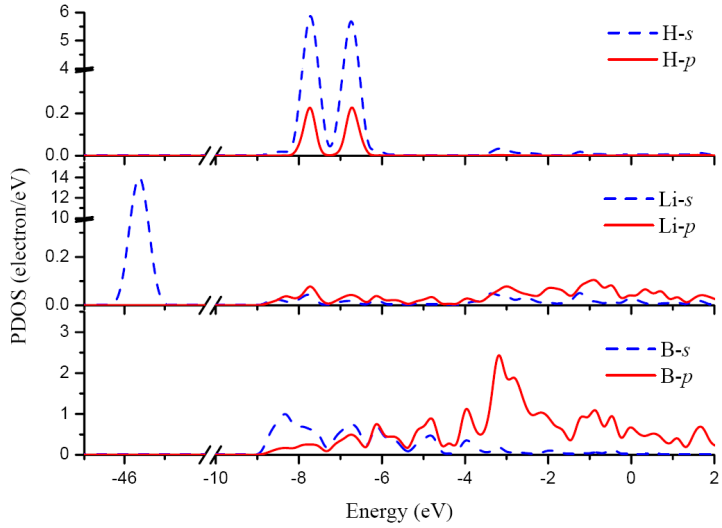

(*b*)

Fig. 7 PDOS of all H atoms, Li atoms and B atoms in (*a*) $(H_2)_2$@Li_2B_5-I and (*b*) $(H_2)_4$@Li_2B_5-I.

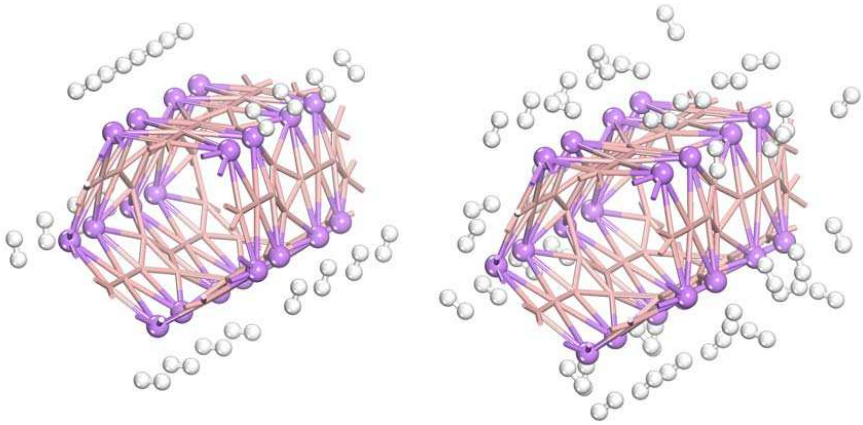

Fig. 8 Optimized configurations of (0,5) nanotube with (*a*) one and (*b*) two H_2 molecules adsorbed onto each Li atom.